



A light-curve analysis of the X-ray flash first observed in classical novae

MARIKO KATO ¹, HIDEYUKI SAIO,² AND IZUMI HACHISU ³¹*Department of Astronomy, Keio University, Hiyoshi, Kouhoku-ku, Yokohama 223-8521, Japan*²*Astronomical Institute, Graduate School of Science, Tohoku University, Sendai 980-8578, Japan*³*Department of Earth Science and Astronomy, College of Arts and Sciences, The University of Tokyo, 3-8-1 Komaba, Meguro-ku, Tokyo 153-8902, Japan*

ABSTRACT

An X-ray flash, expected in a very early phase of a nova outburst, was at last detected with the *SRG*/eROSITA in the classical nova YZ Reticuli 2020. The observed flash timescale, luminosity, and blackbody temperature substantially constrain the nova model. We present light curve models of the X-ray flash for various white dwarf (WD) masses and mass accretion rates. We have found the WD mass in YZ Ret to be as massive as $M_{\text{WD}} \sim 1.3 M_{\odot}$ with mass accretion rates of $\dot{M}_{\text{acc}} \sim 5 \times 10^{-10} - 5 \times 10^{-9} M_{\odot} \text{ yr}^{-1}$ including the case that the mass accretion rate is changing between them, to be consistent with the *SRG*/eROSITA observation. The X-ray observation confirms the luminosity to be close to the Eddington limit at the X-ray flash. The occurrence of optically thick winds, with the photospheric radius exceeding $\sim 0.1 R_{\odot}$, terminated the X-ray flash of YZ Ret by strong absorption. This sets an constrain on the starting time of wind mass loss. A slight contamination of the core material into the hydrogen rich envelope seems to be preferred to explain a very short duration of the X-ray flash.

Keywords: novae, cataclysmic variables — stars: individual (YZ Ret) — stars: winds — stars: X-ray

1. INTRODUCTION

A nova is a thermonuclear runaway event on a mass-accreting white dwarf (WD) (see, e.g., Kato et al. 2022, for a recent self-consistent calculation). A hydrogen-rich envelope on the WD quickly brightens up to $L_{\text{ph}} \sim 10^{38} \text{ erg s}^{-1}$ or several $10^4 L_{\odot}$ just after the start of a runaway of the hydrogen-shell burning. Here, L_{ph} is the photospheric luminosity. In an early phase of expansion of the photosphere, its surface temperature increases up to $T_{\text{ph}} \sim 10^6 \text{ K}$ and the nova emits supersoft X-rays at a rate of $L_X \sim 10^{38} \text{ erg s}^{-1}$. The duration of the bright soft X-ray phase is so short that it is called the “X-ray flash” in the rising phase of a nova. Such X-ray flashes have long been expected to be observed, but no one detected until UT 2020 July 7 when the eROSITA instrument on board *Spectrum-Roentgen-Gamma* (*SRG*) scanned the region of YZ Reticuli (König et al. 2022).

The nova outburst of YZ Ret (Nova Ret 2020) was reported first by McNaught (2020) at visual magni-

tude 5.3 on UT 2020 July 15. This object was known as a cataclysmic variable (MGAB-V207), a novalike VY Scl-type variable with irregular variations in the *V* magnitude range 15.8 – 18.0 mag (Kilkenny et al. 2015). The nova was classified as a He/N-type by Carr et al. (2020). The distance to the nova is estimated to be $d = 2.53^{+0.52}_{-0.26} \text{ kpc}$ by Bailer-Jones et al. (2021) based on the *Gaia*/eDR3 data. The galactic coordinates are $(\ell, b) = (265^{\circ}3975, -46^{\circ}3954)$ (ep=J2000), so the nova is located at 1.8 kpc below the galactic disk. The galactic absorption toward YZ Ret is as low as $E(B - V) \sim 0.03$ (Sokolovsky et al. 2022). The orbital period was obtained by Schaefer (2022) to be $P_{\text{orb}} = 0.1324539 \pm 0.0000098 \text{ days}$ (=3.17889 hr). Thanks to the short distance $d = 2.5 \text{ kpc}$ from the Earth and very low galactic absorption $E(B - V) \sim 0.03$, the nova was observed in muti-wavelengths, including optical, X-ray, and gamma-ray from a very early phase of the outburst until a very later phase through a supersoft X-ray source (SSS) phase. X-ray and γ -ray observations are reported by Sokolovsky et al. (2022) and König et al. (2022).

The most remarkable characteristic of YZ Ret observation is the detection of an X-ray flash. This is the

first positive detection among any types of nova outbursts. König et al. (2022) reported the X-ray flash on UT 2020 July 7 observed with the *SRG*/eROSITA. This detection is serendipitous during its all sky survey. Since the X-ray flash of a nova is a brief phenomenon that occurs before the optical brightening, it is not possible to exactly predict when it occurs.

Historically, there were a few attempts for detecting an X-ray flash. Morii et al. (2016) searched MAXI data for X-ray flashes that would possibly occurred during the MAXI survey at the position and time of known nova outbursts, but unsuccessful. Kato et al. (2016) attempted to detect an X-ray flash just before the expected nova outbursts of one-year-period recurrent nova M31N 2008-12a. This was the first planned observation, but no X-ray flash was detected in its 2015 outburst.

Theoretical models predict X-ray flashes detectable only for a very short time ($\lesssim 1$ day) depending on the WD mass and mass-accretion rate (Kato et al. 2016). In low mass WDs, the surface temperature does not rise as high as to emit much X-rays, and most of photon energy is far-UV instead of X-ray (e.g., Kato et al. 2017, 2022). Thus, the X-ray flash should be detectable only in massive WDs. The time interval between the X-ray flash and optical maximum also depends on the WD mass and mass-accretion rate, which is, however, poorly understood. A very early phase, before a nova brightens optically, is one of the frontiers in nova studies. Because no planned observations had been successful, only the serendipitous detection of the X-ray flash with the *SRG*/eROSITA gives us invaluable information on the very early phase of a nova.

In this paper, we present theoretical light curve models of X-ray flashes, the duration of which are short enough to match the *SRG*/eROSITA observation. Only massive WDs are responsible for the flash like in YZ Ret.

This paper is organized as follows. Section 2 presents our numerical method and results for the X-ray flash, and compares them with the observational data for YZ Ret. Conclusions follow in section 3.

2. MODEL CALCULATION OF X-RAY FLASH

We have calculated models of nova outbursts with a Henyey type time-dependent code combined with steady-state optically thick wind solutions. The numerical method is the same as that in Kato et al. (2022). We list our model parameters in Table 1. From left to right, model name, WD mass, mass accretion rate, additional carbon mixture in the hydrogen-rich envelope, recurrence period of nova outbursts, starting time of winds since the onset of thermonuclear runaway, maximum nuclear burning rate that represents the strength of a flash,

ignition mass, and pass or not the requirement from the scan detection. The $1.0 M_{\odot}$ WD model (Model A) is taken from Kato et al. (2022). The mass accretion rate $\dot{M}_{\text{acc}} = 5 \times 10^{-9} M_{\odot} \text{ yr}^{-1}$ is close to the median value in the distribution of mass-accretion rates for classical novae obtained by Selvelli & Gilmozzi (2019) while the mass accretion rate $\dot{M}_{\text{acc}} = 5 \times 10^{-10} M_{\odot} \text{ yr}^{-1}$ is close to the empirical rate (Knigge et al. 2011) for cataclysmic variable systems with an orbital period of $P_{\text{orb}} = 3.18$ hr. Since many old novae are observed to fade significantly on timescales of ~ 100 years (e.g., Duerbeck 1992; Johnson et al. 2014), we have taken into account a gradual decrease of accretion rate in Model H, in which accretion resumes at a rate of $\dot{M}_{\text{acc}} = 5 \times 10^{-9} M_{\odot} \text{ yr}^{-1}$ just after the end of a previous flash, while the accretion rate gradually decreases.

We have assumed solar composition for accreted matter ($X = 0.7$, $Y = 0.28$, and $Z = 0.02$) for all the models except Model J. In many classical novae, heavy element enrichment is observed in the ejecta (e.g., Gehrz et al. 1998). To mimic such a heavy element enrichment one may replace the envelope composition with that polluted by the WD core composition at the onset of thermonuclear runaway (e.g., Starrfield et al. 2020), or assume a CO enhancement in the accreting matter (e.g., Chen et al. 2019). In Model E, F, G, H, and I we have increased carbon mass fraction by 0.1 and decreased helium mass fraction by the same amount at the onset of thermonuclear runaway. In Model J, we have assumed carbon rich mixture ($X = 0.6$, $Y = 0.28$, $X_{\text{C}} = 0.1$, and $Z = 0.02$) for accreting matter.

2.1. Cycle of nova evolution in the HR diagram

Figure 1 shows one cycle of nova outbursts for a $1.0 M_{\odot}$ WD (Model A) and $1.35 M_{\odot}$ WD (Model I) in the HR diagram. In the quiescent phase (inter outburst period), the accreting WD stays around the bottom of each loop. After the thermonuclear runaway sets in, the WD goes upward keeping the photospheric radius almost constant. The photospheric temperature increases to maximum, $\log T_{\text{ph}}^{\text{max}}$ (K)=5.58 in the $1.0 M_{\odot}$ model (Model A) and 6.02 in the $1.35 M_{\odot}$ model (Model I). In these high temperature phases, the WD photosphere emits X-ray/UV photons, which corresponds to an X-ray/UV flash. After that, the envelope expands and the photospheric temperature begins to decrease. Optically thick winds start when the envelope expands and the surface temperature decreases to $\log T_{\text{ph}}$ (K)=5.32 in the $1.0 M_{\odot}$ model and 5.46 in the $1.35 M_{\odot}$ model (at each open circle).

Table 1. Nova Models

| Model | | M_{WD} | \dot{M}_{acc} | C mix | t_{rec} | t_{ML}^a | $L_{\text{nuc}}^{\text{max}}$ | M_{ig} | comment |
|----------------|-----|-----------------|---------------------------------|------------------|------------------|-------------------|-------------------------------|-------------------------|--------------------------|
| | | (M_{\odot}) | ($M_{\odot} \text{ yr}^{-1}$) | | (yr) | (hr) | ($10^8 L_{\odot}$) | ($10^{-5} M_{\odot}$) | pass or not ^b |
| A ^c | ... | 1.0 | 5×10^{-9} | no | 5400 | 25 | 2.3 | 3.0 | Fig.3a,no |
| B | ... | 1.2 | 5×10^{-9} | no | 1500 | 18 | 3.6 | 0.82 | Fig.3b,no |
| C | ... | 1.35 | 5×10^{-9} | no | 220 | 6.1 | 3.3 | 0.13 | Fig.3c,no |
| D | ... | 1.35 | 5×10^{-10} | no | 2900 | 4.0 | 8.6 | 0.16 | Fig.3d,pass |
| E | ... | 1.3 | 5×10^{-9} | yes ^d | 300 | 3.2 | 16 | 0.16 | Fig.3e,pass |
| F | ... | 1.3 | 5×10^{-10} | yes ^d | 4600 | 1.5 | 74 | 0.25 | Fig.3f,pass |
| G | ... | 1.35 | 5×10^{-9} | yes ^d | 120 | 1.8 | 12 | 0.070 | Fig.3g,pass |
| H | ... | 1.35 | Decreasing ^e | yes ^d | 1700 | 1.1 | 63 | 0.10 | Fig.3h,pass |
| I | ... | 1.35 | 5×10^{-10} | yes ^d | 1900 | 1.5 | 60 | 0.10 | Fig.3i,pass |
| J | ... | 1.35 | 5×10^{-10} | yes ^f | 1200 | 2.9 | 3.6 | 0.066 | ...,pass |

^a Starting time of optically thick winds since the L_{nuc} peak ($t = 0$).

^b pass or not the detection requirement of 22nd (no), 23rd (yes), and 24th (no) scan.

^c Model taken from Kato et al. (2022).

^d Increased carbon mass-fraction by 0.1 at ignition.

^e Mass accretion rate is changing from 5×10^{-9} to $5 \times 10^{-10} M_{\odot} \text{ yr}^{-1}$.

^f Mass accretion of carbon rich matter by 0.1.

The filled red circle with error bars indicates the position of the X-ray flash of YZ Ret observed by *SRG/eROSITA*. The point lies on the evolution track of Model I ($1.35 M_{\odot}$) just before optically thick winds start, which is important because the winds possibly self-absorb soft X-rays as discussed in the next subsection.

When the photospheric radius attains its maximum expansion, the wind mass loss rate also reaches maximum. The hydrogen-rich envelope mass quickly decreases mainly due to wind mass loss. The photospheric radius begins to shrink while the photospheric temperature turns to increase. In a later phase, optically thick winds stop (at each open square) and the photospheric temperature becomes as high as $\log T_{\text{ph}} \text{ (K)} = 5.5 - 6.1$ and the WD again emits X-ray/UV photons. This phase is called the supersoft X-ray source (SSS) phase in the decay phase of a nova outburst.

The wind phase after the optical maximum and following SSS phase have been observed well in a number of nova outbursts. However, an early phase before the optical maximum has rarely been studied.

2.2. Optically thick winds absorb X-rays

Figure 2 shows a close up view of the rising phase on the HR diagram. The optically thick winds starts at the open circles on each line. The wind phase is denoted by the dotted line. The optically thick winds would absorb

and strongly weaken the X-ray flux. The optical depth for X-ray is estimated from equation (9) of Li et al. (2017) as

$$\tau_X \approx 8 \times 10^3 \left(\frac{\dot{M}_{\text{wind}}}{10^{-7} M_{\odot} \text{ yr}^{-1}} \right) \left(\frac{r}{10^{10} \text{ cm}} \right)^{-1} \times \left(\frac{v_{\text{wind}}}{400 \text{ km s}^{-1}} \right)^{-1} \left(\frac{E_X}{\text{keV}} \right)^{-2}. \quad (1)$$

Parameters of our models soon after the start of winds are, $R_{\text{ph}} \sim 10^{10} \text{ cm}$ and $\dot{M}_{\text{wind}} \sim 10^{-7} M_{\odot} \text{ yr}^{-1}$. Using these values in equation (1), we find the optical depth of X-ray in the winds to be as high as $\tau_X \sim 10^6$ for $E_X \sim 0.1 \text{ keV}$. Thus, soft X-ray emission would be absorbed in the wind phase. In other words, the X-ray flash could be terminated by the start of the winds.

König et al. (2022) fitted the X-ray spectrum of YZ Ret with a blackbody spectrum and obtained $T_{\text{BB}} = 3.27_{-0.33}^{+0.11} \times 10^5 \text{ K}$ ($kT_{\text{BB}} = 28.2_{-2.8}^{+0.9} \text{ eV}$). They also derived absolute luminosity to be $L_{\text{ph}} = (2.0 \pm 1.2) \times 10^{38} \text{ erg s}^{-1}$. These estimates are plotted in Figure 2 by an open red circle with error bars. The estimated blackbody flux has a large error bar, but it is consistent only with relatively massive WDs ($M_{\text{WD}} \gtrsim 1.2 M_{\odot}$).

The estimated blackbody temperature is located left-side the open circles, that is, before optically thick winds start. Thus, theoretically, no strong emission lines are expected. This is consistent with no prominent emis-

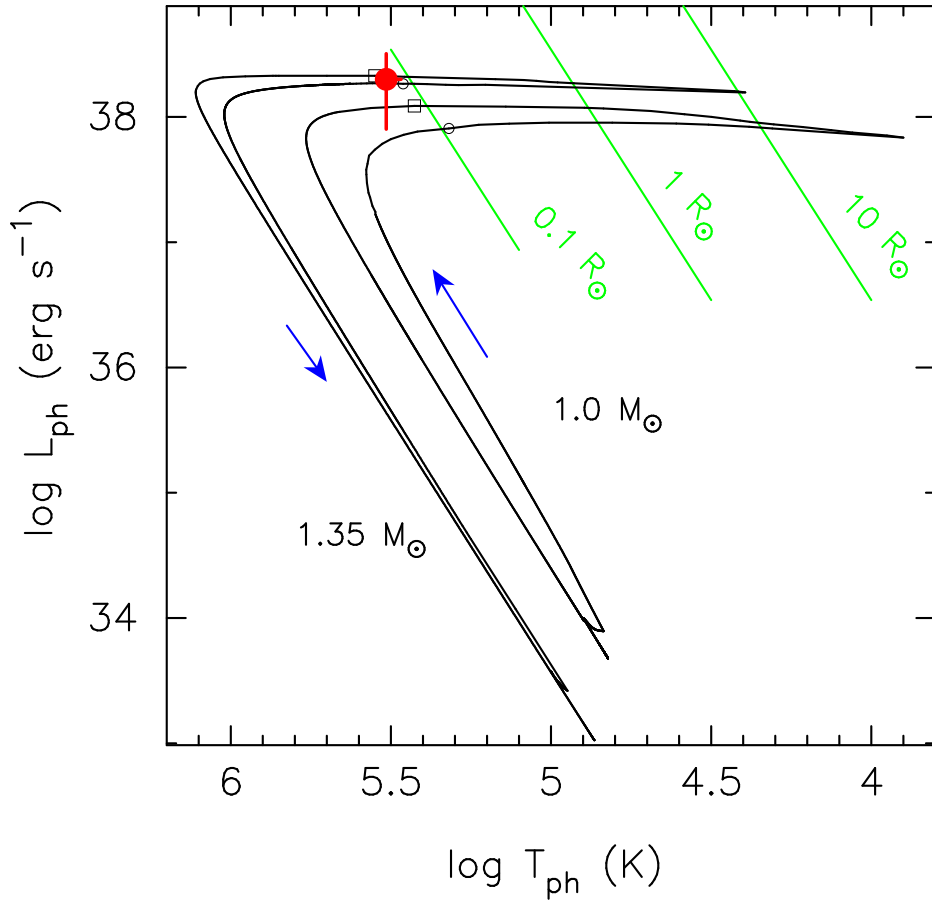


Figure 1. Comparison of nova outbursts in the HR diagram between a $1.0 M_{\odot}$ white dwarf (WD) (Model A) and $1.35 M_{\odot}$ WD (Model I), where L_{ph} and T_{ph} are the photospheric luminosity and temperature, respectively. The green lines show equi-radius lines, the value of which is attached beside each line, based on the relation of $L_{\text{ph}} = 4\pi R_{\text{ph}}^2 \sigma T_{\text{ph}}^4$, where R_{ph} and σ are the photospheric radius and Stefan-Boltzmann constant, respectively. Each arrow indicates the direction of evolution. The filled red circle with error bars corresponds to the X-ray flash in YZ Ret (König et al. 2022). The open circles indicate the start of optically thick winds while the open squares represent the end of winds.

sion lines in the observed X-ray spectrum (König et al. 2022).

Sokolovsky et al. (2022) estimated the galactic hydrogen column density to be $1 \times 10^{19} \text{ cm}^{-2} \lesssim N_{\text{H}} \lesssim 1.86 \times 10^{20} \text{ cm}^{-2}$. König et al. (2022) obtained $N_{\text{H}} < 1.4 \times 10^{20} \text{ cm}^{-2}$ toward the nova based on their X-ray spectrum analysis and concluded that there is no major intrinsic absorption during the X-ray flash. Such small hydrogen column density is consistent with our models in which the optically thick winds are absent at the stage of $kT_{\text{ph}} = 28.2 \text{ eV}$.

2.3. Very short duration of X-ray flash

König et al. (2022) reported that the *SRG/eROSITA* scanned the region of YZ Ret 28 times (every 4 hours) and detected YZ Ret at the 23rd scan for about 36 s but did not detect 4 hours before and after this scan. This

means that the duration of X-ray flash is shorter than 8 hours.

Figure 3 shows the X-ray light curves during the flash for our models in Table 1 except model J. The black lines correspond to the 0.2-10 keV band of the *SRG/eROSITA* instrument while the red lines indicate the temporal variations of photospheric temperature. The open circle on each black line indicates the start of optically thick winds. The dotted line extending from the open circle indicates the evolution path with the winds, during which no significant X-ray flux is expected. The large black dot with error bars on each red line shows the epoch when the photospheric temperature decreases to $kT_{\text{ph}} = 28.2^{+0.9}_{-2.8} \text{ eV}$. The large red dot on each black line corresponds to the X-ray luminosity at this epoch. Two vertical green arrows indicate 4 hours before/after this epoch. The X-ray luminosity at the epochs of arrows should be smaller than that at

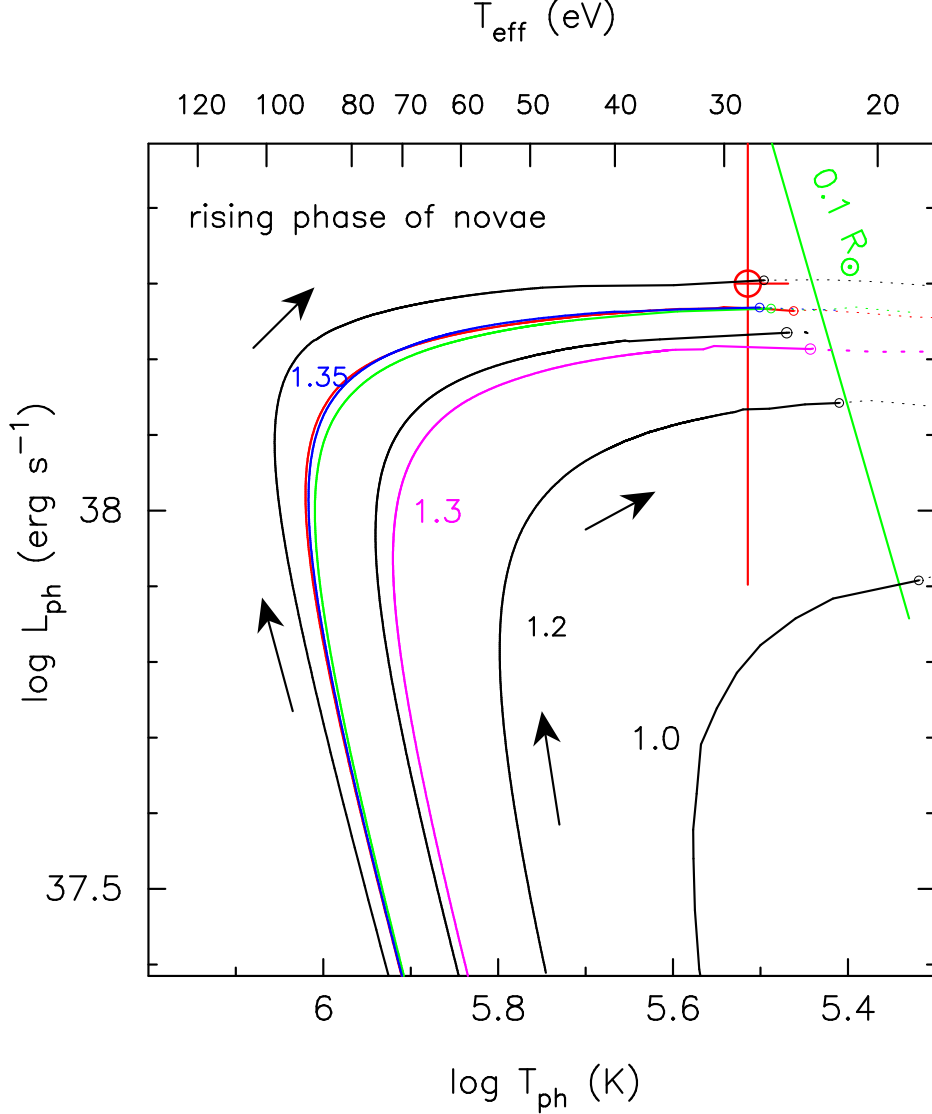


Figure 2. Close up view only of the rising phases of novae in the HR diagram. Optically thick winds start at the open circles on each track. The track rightside the open circle (low temperature side) corresponds to the wind phase, denoted by a dotted line. Each model corresponds to those in Table 1, from upper to lower, black line (Model J), red (I), blue (C), and green (D), all for $1.35 M_{\odot}$ WDs, Model E (black) and F (magenta) for $1.3 M_{\odot}$, B ($1.2 M_{\odot}$: black), and A ($1.0 M_{\odot}$: black). The red dot with the error bars denotes $kT_{\text{ph}} = 28.2^{+0.9}_{-2.8}$ eV, $L_{\text{ph}} = (2.0 \pm 1.2) \times 10^{38}$ erg s $^{-1}$, and radius $R_{\text{ph}} = 50000 \pm 18000$ km ($= 0.07 \pm 0.026 R_{\odot}$) estimated for YZ Ret (König et al. 2022).

the red dot by four orders of magnitude because the *SRG*/eROSITA did not detect X-rays.

Model A, B, and C evolve slowly, and should have detectable X-ray fluxes even before and/or after four hours of the detection epoch by the *SRG*/eROSITA, contradicting with the non-detection. The upward (downward) arrow indicates the theoretical prediction of detectable (non-detectable) X-ray flux. Model D is marginally consistent with the requirement.

The carbon mixture models evolve much faster and easily fulfill the requirements. The CNO enrichment in the hydrogen rich envelope make flash evolution faster

because the CNO reaction rates increase. A faster evolution is favorable to be consistent with the constraints from the observation of *SRG*/eROSITA. Furthermore, the appearance of the optically thick winds would contribute to shorten the duration of the X-ray flash of YZ Ret.

In Model H the mass accretion restarts after a shell flash ends with a rate of $\dot{M}_{\text{acc}} = 5 \times 10^{-9} M_{\odot} \text{ yr}^{-1}$ which gradually decreases to $5 \times 10^{-10} M_{\odot} \text{ yr}^{-1}$ in the first 100 years of the quiescent phase and keep constant after that. Until the next outburst, long after 1600 years, the WD thermal structure is adjusted to the lower accretion

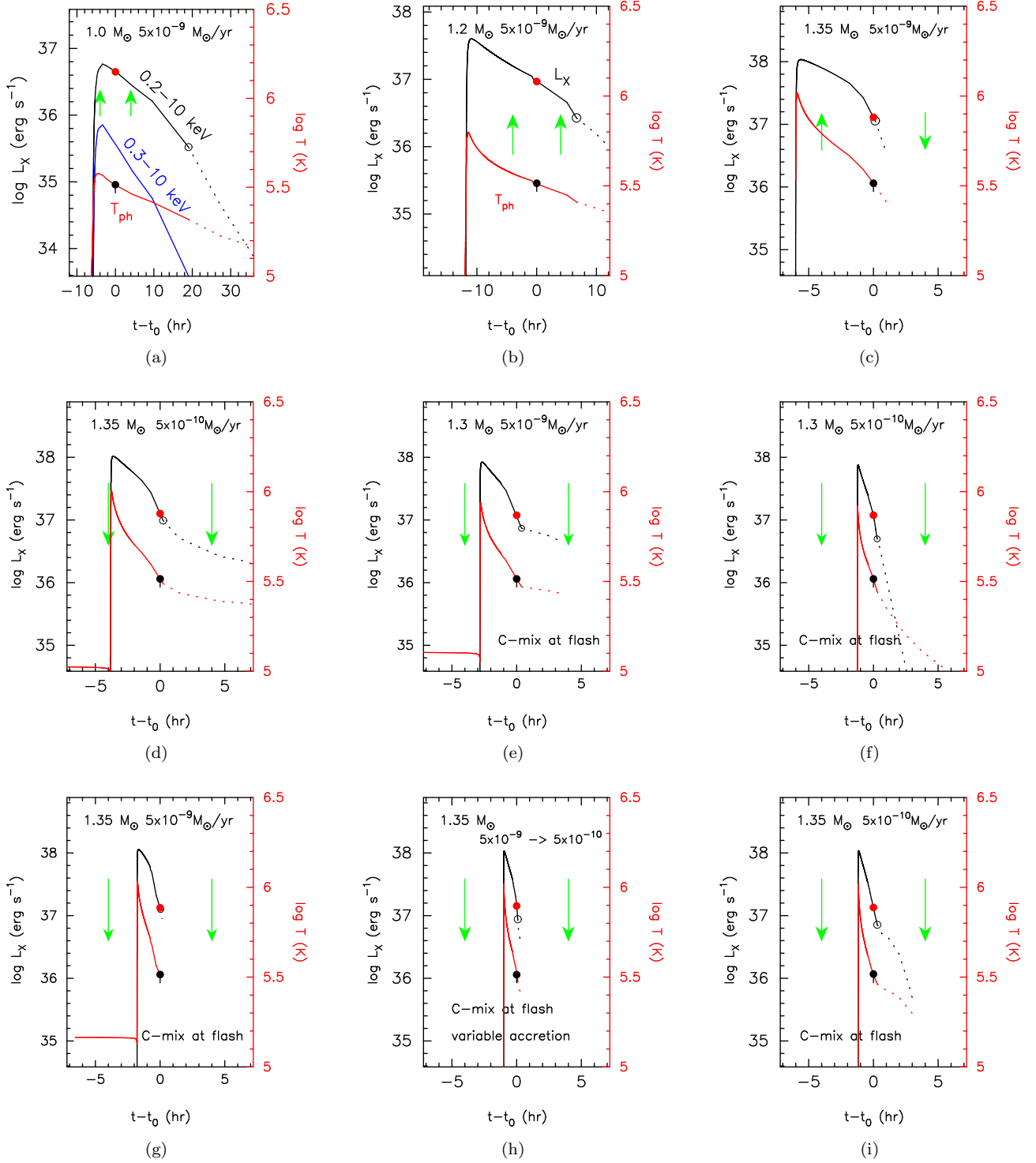


Figure 3. X-ray light curves for the X-ray flash models. Each panel corresponds to each model in Table 1. The red lines are the temporal variations of the photospheric temperature, T_{ph} , which are scaled on the right side vertical axis printed in red. The black lines show the estimated 0.2-10 keV (*SRG*/eROSITA) band flux while the blue line in panel (a) indicates the (0.3-10) keV (*Swift*/XRT) band flux. They are scaled on the left vertical axis. Each open circle on the black lines corresponds to the epoch when winds start. The dotted part means a wind phase. The large red dots on each black line show the X-ray luminosity at the epoch of $kT_{ph} = 28.2$ eV ($\log T_{ph}$ (K) = 5.515), corresponding to the observed blackbody temperature of the YZ Ret flash. The origin of time denoted by t_0 is the observed time with the *SRG*/eROSITA at the 23rd scan. The two green arrows indicate 4 hours before (22nd scan) and after (24th scan) the observation (23rd scan).

rate. As a result the outburst properties should be similar to a model of mass accretion rate of $5 \times 10^{-10} M_{\odot} \text{ yr}^{-1}$. Model H shows in fact similar properties to model I, but slightly stronger flash properties, i.e., shorter flash duration and larger $L_{\text{nuc}}^{\text{max}}$ than in Model I.

König et al. (2022) also reported that the X-ray flux of YZ Ret decreased by about a few to 10% even during the very short 36 s observation period. We estimate X-ray decay rates of our models to find a few % in Model F, G, H, and I during a 30 s period near the point denoted by the large red dot, being broadly consistent with the observation.

YZ Ret is a novalike VY Scl-type star, in which dwarf nova outbursts are suppressed. To suppress thermal disk instability of a dwarf nova, the mass transfer rate is higher than \dot{M}_{crit} . This critical rate is estimated to be $\dot{M}_{\text{crit}} \sim 2 \times 10^{-9} M_{\odot} \text{ yr}^{-1}$ for $P_{\text{orb}} = 3.18$ hr and an assumed total binary mass of $M_1 + M_2 \sim 1.3 + 0.3 = 1.6 M_{\odot}$ (see, e.g., equations (3) and (4) of Osaki 1996). Our Model E and G (1.3 and 1.35 M_{\odot} WD models with a relatively high mass accretion rate of $\dot{M}_{\text{acc}} = 5 \times 10^{-9} M_{\odot} \text{ yr}^{-1}$) satisfy this requirement of novalike stars, i.e., $\dot{M}_{\text{acc}} > \dot{M}_{\text{crit}}$.

We should emphasize the importance of low energy sensitivity of detector. The blue line in Figure 3a shows an X-ray light curve of the 0.3-10 keV band corresponding to the *Swift*/XRT. The flux is about ten times smaller than the *SRG*/eROSITA flux (0.2-10 keV band), clearly showing that, for an efficient detection of X-ray flashes, the low energy sensitivity (down to 0.2 keV or lower) is important.

2.4. Clue to the origin of the super-Eddington luminosity

We should remark the importance of the X-ray flash on the super-Eddington problem in novae. The bolometric luminosity of a star in hydro-static balance cannot exceed the Eddington limit as long as spherical symmetry is assumed. The Eddington limit is defined by

$$L_{\text{Edd}} \equiv \frac{4\pi c G M_{\text{WD}}}{\kappa} = 2 \times 10^{38} \text{ erg s}^{-1} \left(\frac{1.7}{1+X} \right) \left(\frac{M_{\text{WD}}}{1.4 M_{\odot}} \right) \quad (2)$$

for massive WDs with the mass of M_{WD} , where $\kappa = 0.2(1+X) \text{ cm}^2 \text{ g}^{-1}$ is the electron scattering opacity.

YZ Ret reached its optical peak $V = 3.7$ four days after the X-ray flash (McNaught & Phillips 2020). This brightness corresponds to an absolute V magnitude of $M_V = 3.7 - (m - M)_V = -8.4$, which is several times

larger than the Eddington limit.¹ Here, the distance modulus in V band is estimated to be $(m - M)_V = 5 \log(d/10 \text{ pc}) + A_V = 12.0 + 0.1 = 12.1$.

At the X-ray flash of YZ Ret, however, the total photospheric luminosity was estimated to be $L_{\text{ph}} = (2.0 \pm 1.2) \times 10^{38} \text{ erg s}^{-1}$ (König et al. 2022). Thus, the photospheric luminosity did not largely exceed the Eddington limit (see Figures 1 and 2). This clearly confirms that the nova envelope is in hydro-static balance at the X-ray flash, when the optically thick winds had not yet started. Thus, we may conclude that the origin of super-Eddington luminosity is closely related to the occurrence of optically thick winds.

3. CONCLUSIONS

An X-ray flash in the rising phase of a nova was first detected in the classical nova YZ Ret, which provides us with invaluable information for the nova physics. We may conclude our theoretical analysis as follows.

- König et al. (2022) found X-ray spectrum at the flash to be consistent with an unabsorbed blackbody of $3 \times 10^5 \text{ K}$. This is consistent with our hydrostatic evolution models just before optically thick winds start.
- The blackbody temperature $T_{\text{BB}} \approx 3 \times 10^5 \text{ K}$ and luminosity of $L_{\text{ph}} \approx 2 \times 10^{38} \text{ erg s}^{-1}$ are consistent with our models of very massive WDs ($M_{\text{WD}} \gtrsim 1.2 M_{\odot}$).
- The very short duration of the X-ray flash ($\lesssim 8$ hr) further constrains the mass of WD ($M_{\text{WD}} \gtrsim 1.3 M_{\odot}$), depending on the degree of WD core material mixing into the hydrogen-rich envelope. The generation of optically thick winds when the photospheric radius exceeds $\sim 0.1 R_{\odot}$ might terminate the X-ray flash of YZ Ret.
- YZ Ret is a novalike VY Scl-type star, which requires a relatively high mass accretion rate ($\gtrsim \dot{M}_{\text{crit}} \sim (2-3) \times 10^{-9} M_{\odot} \text{ yr}^{-1}$) to suppress dwarf nova outbursts. If it is the case, our 1.3 and 1.35 M_{\odot} WD models with a relatively high mass accretion rate of $\dot{M}_{\text{acc}} = 5 \times 10^{-9} M_{\odot} \text{ yr}^{-1}$ (Model E and G) satisfy the requirement of $\dot{M}_{\text{acc}} > \dot{M}_{\text{crit}}$.
- The nova envelope is in hydro-static balance at the X-ray flash, just before optically thick winds

¹ The bolometric magnitude is $M_{\text{bol}} = -7.07$ for $L_{\text{ph}} = 2 \times 10^{38} \text{ erg s}^{-1}$. This corresponds to $M_V \approx -7.0$ or -6.0 for the bolometric correction B.C. = -0.07 (8700 K) or B.C. = -1.07 (14000 K), for example. Then the flux ratio is $10^{(8.4-7.0)/2.5} \approx 4$ or $10^{(8.4-6.0)/2.5} \approx 9$ (times the Eddington limit).

start. In a few days later, the optical luminosity highly exceeds the Eddington limit. This suggests that the origin of super-Eddington luminosity is closely related to the occurrence of optically thick winds.

We are grateful to the anonymous referee for useful comments, which improved the manuscript.

REFERENCES

- Bailer-Jones, C. A. L., Rybizki, J., Fouesneau, M., Demleitner, M., & Andrae, R. 2021, *AJ*, 161, 147, <https://doi.org/10.3847/1538-3881/abd806>
- Carr, A., Said, K., Davis, T. M., Lidman, C., & Tucker, B. E. 2020, *ATel*, No. 13874
- Chen, H.-L., Woods, T. E., Yungelson, L. R., et al. 2019, *MNRAS*, 490, 1678, <https://doi.org/10.1093/mnras/stz2644>
- Duerbeck, H. W. 1992, *MNRAS*, 258, 629, <https://doi.org/10.1093/mnras/258.3.629>
- Gehrz, R. D., Truran, J. W., Williams, R. E., & Starrfield, S. 1998, *PASP*, 110, 3, <https://doi.org/10.1086/316107>
- Johnson, C. B., Schaefer, B. E., Croll, P., & Henden, A. A. 2014, *ApJ*, 780, L25, <https://doi.org/10.1088/2041-8205/780/2/L25>
- Kato, M., Saio, H., & Hachisu, I., 2017, *ApJ*, 838, 153, <https://doi.org/10.3847/1538-4357/838/2/153>
- Kato, M., Saio, H., & Hachisu, I. 2022, *PASJ*, in press (arXiv:2206.03136v2), <https://doi.org/10.1093/pasj/psac051>
- Kato, M., Saio, H., Henze, M. et al. 2016, *ApJ*, 830, 40, <https://doi.org/10.3847/0004-637X/830/1/40>
- König, O., Wilms, J., Arcodia, R., et al. 2022, *Nature*, 605, 248, <https://doi.org/10.1038/s41586-022-04635-y>
- Kilkenny, D., O'Donoghue, D., Worters, H. L. et al. 2015, *MNRAS*, 453, 1879, <https://doi.org/10.1093/mnras/stv1771>
- Knigge, C., Baraffe, I., & Patterson, J. 2011, *ApJS*, 194, 28, <https://doi.org/10.1088/0067-0049/194/2/28>
- Li, K.-L., Metzger, B. D., Chomiuk, L., et al. 2017, *Nature Astronomy*, 1, 697, <https://doi.org/10.1038/s41550-017-0222-1>
- McNaught, R. H. 2020, *CBET*, No.4811, 1
- McNaught, R. H., & Phillips, M. A. 2020, *CBET*, No.4812, 2
- Morii, M., Yamaoka, H., Mihara, T., Matsuoka, M., & Kawai, N. 2016, *PASJ*, 68, S11, <https://doi.org/10.1093/pasj/psw007>
- Osaki, Y. 1996, *PASP*, 108, 39, <https://doi.org/10.1086/133689>
- Schaefer, B. E. 2022, *MNRAS*, in press (arXiv:2207.02932)
- Selvelli, P., & Gilmozzi, R. 2019, *A&A*, 622, A186, <https://doi.org/10.1051/0004-6361/201834238>
- Sokolovsky, K. V., Li, K.-L., Lopes de Oliveira, R., et al. 2022, *MNRAS*, 514, 2239, <https://doi.org/10.1093/mnras/stac1440>
- Starrfield, S., Bose, M., Iliadis, C. et al. 2020, *ApJ*, 895, 70, <https://doi.org/10.3847/1538-4357/ab8d23>